A second-order accurate semi-implicit δf method for kinetic MHD simulation

Jianhua Cheng, Yang Chen, Scott E. Parker, Dmitri Uzdensky

University of Colorado-Boulder

Outline

1. Motivation
   - The Lorentz force ions are needed in cases where the gyro-kinetic orderings are not valid (edge pedestal, reconnection without guide field).
   - The hybrid model is suitable for studying the relatively low frequency phenomena and includes full ion kinetic effects.
2. The model, equations and numerics
   - Ion equations of motion, field equations, the generalized Ohm's law.
   - The second-order accuracy implicit δf method.
3. Simulations
   - Alfven waves, whistler waves and ion sound waves in a slab.
   - The resistive tearing mode for Harris sheet equilibrium configuration.
4. Summary

Ion equations of motion and field equations

- Lorentz force ions

$$\frac{d\boldsymbol{v}_i}{dt} = \frac{q_i}{m_i}(\boldsymbol{E} + \boldsymbol{v}_i \times \boldsymbol{B})$$
$$\frac{d\boldsymbol{x}_i}{dt} = \boldsymbol{v}_i$$

- Ampere's equation

$$\bigtriangledown \times \boldsymbol{B} = \mu_0 \left(n_i q_i \boldsymbol{u}_i - n_e e \boldsymbol{u}_e\right)$$

- Faraday's law

$$\bigtriangledown \times \boldsymbol{E} = -\frac{\partial \boldsymbol{B}}{\partial t}$$

The generalized Ohm's law

- Starting from the electron momentum equation:

$$en_e(\boldsymbol{E} + \boldsymbol{u}_e \times \boldsymbol{B}) = en_e\eta\, \boldsymbol{j} - \bigtriangledown \cdot \boldsymbol{\Pi}_e - m_e \frac{\partial(n_e \boldsymbol{u}_e)}{\partial t}$$

where $\boldsymbol{\Pi}_e = \int f_e m_e \boldsymbol{v}\boldsymbol{v} d\boldsymbol{v}$.

- Substitute in Ampere's equation $\boldsymbol{j} = (n_i q_i \boldsymbol{u}_i - n_e e \boldsymbol{u}_e) = \frac{1}{\mu_0} \bigtriangledown \times \boldsymbol{B}$, the above equation could be rewritten as

$$en_e\boldsymbol{E} = -\boldsymbol{j}_i \times \boldsymbol{B} + \frac{1}{\mu_0}(\bigtriangledown \times \boldsymbol{B}) \times \boldsymbol{B} + \frac{en_e}{\mu_0}\eta\,(\bigtriangledown \times \boldsymbol{B}) - \bigtriangledown \cdot \boldsymbol{\Pi}_e - m_e \frac{\partial(n_e \boldsymbol{u}_e)}{\partial t}$$

where $\boldsymbol{j}_i = n_i q_i \boldsymbol{u}_i$.

Electron inertial

- Taking time derivative of Ampere's equation

$$\mu_0 \left(q_i \frac{\partial n_i \boldsymbol{u}_i}{\partial t} - e \frac{\partial n_e \boldsymbol{u}_e}{\partial t} \right) = \bigtriangledown \times \frac{\partial \boldsymbol{B}}{\partial t} = - \bigtriangledown \times \bigtriangledown \times \boldsymbol{E}$$

- By treating the first term on the left hand side using the ion momentum equation, we could write the electron inertial term as

$$m_e \frac{\partial (n_e \boldsymbol{u}_e)}{\partial t} = \frac{m_e}{m_i} \frac{q_i}{e} \left(q_i n_i (\boldsymbol{E} + \boldsymbol{u}_i \times \boldsymbol{B}) - \bigtriangledown \cdot \boldsymbol{\Pi}_i - q_i n_i \frac{\eta}{\mu_0} \bigtriangledown \times \boldsymbol{B} \right) + \frac{m_e}{\mu_0 e} \bigtriangledown \times \bigtriangledown \times \boldsymbol{E}.$$

The generalized Ohm's law and electron modeling

- Using quasi-neutrality $n_i = n_e$, the electron density and flow can be calculated directly from particle ions

$$
\begin{aligned}
& en_i(1 + \frac{m_e}{m_i}\frac{q_i^2}{e^2})\boldsymbol{E} + \frac{m_e}{\mu_0 e} \bigtriangledown \times (\bigtriangledown \times \boldsymbol{E}) \\
= & -(1 + \frac{m_e}{m_i}\frac{q_i}{e})\, \boldsymbol{j}_i \times \boldsymbol{B} + \frac{1}{\mu_0}(\bigtriangledown \times \boldsymbol{B}) \times \boldsymbol{B} \\
& + \eta \frac{en_i}{\mu_0}(1 + \frac{m_e}{m_i}\frac{q_i^2}{e^2}) \bigtriangledown \times \boldsymbol{B} - \bigtriangledown \cdot \boldsymbol{\Pi}_e + \frac{m_e}{m_i}\frac{q_i}{e} \bigtriangledown \cdot \boldsymbol{\Pi}_i,
\end{aligned}
$$

- In general, we need an electron model to calculate Π_e. Here we assume the electrons are isothermal and Π_e reduces to

$$P_e = n_e T_e = n_i T_e$$

Future plans include drift-kinetic and gyro-kinetic electron models.

The second-order semi-implicit δf algorithm

- In order to eliminate the fast compressional wave, a second-order semi-implicit method has been implemented.

- For particle ions, the usual δf method is employed. Given a distribution function $f = f_0 + \delta f$, if a weight of $w_j = \frac{\delta f}{f}|_{x=x_j, v=v_j}$ is assigned to each particle, we could then calculate the field quantities by weight δf to the grids. According to Vlasov equation, the particle weight evolves as

$$\frac{d}{dt} w_j = -\frac{d \ln f_0}{dt}|_{x=x_j, v=v_j}$$

Yang Chen, Scott E. Parker, Phys. Plasmas **16**, 052305 (2009)

Normalization and the numerical layout

- The velocity, length and time are normalized to $c_s^2 = T_e/m_i$, $\rho_s = m_i c_s/eB_0$ and $\Omega_{ci}^{-1} = m_i/eB_0$. $\beta_e = \mu_0 n_0 T_e/B_0^2$ is defined upon the uniform background plasma.
- The equations of motion are

$$\frac{\boldsymbol{x}^{n+1} - \boldsymbol{x}^n}{\Delta t} = (1-\theta)\ \boldsymbol{v}^n + \theta\ \boldsymbol{v}^{n+1},$$
$$\frac{\boldsymbol{v}^{n+1} - \boldsymbol{v}^n}{\Delta t} = (1-\theta)\ \boldsymbol{a}^n + \theta\ \boldsymbol{a}^{n+1},$$
$$\frac{w^{n+1} - w^n}{\Delta t} = -(1-\theta)\ (\boldsymbol{v}^n \cdot \bigtriangledown + \boldsymbol{a}^n \cdot \partial_{\boldsymbol{v}}) \ln f_0(\boldsymbol{x}^n, \boldsymbol{v}^n)$$
$$-\theta\ (\boldsymbol{v}^{n+1} \cdot \bigtriangledown + \boldsymbol{a}^{n+1} \cdot \partial_{\boldsymbol{v}}) \ln f_0(\boldsymbol{x}^{n+1}, \boldsymbol{v}^{n+1}),$$

where $\boldsymbol{a} = \frac{q_i}{m_i}(\boldsymbol{E} + \boldsymbol{v} \times \boldsymbol{B})$.

- Generalized Ohm's law:

$$\begin{aligned}
&(n_{i0} + \delta n_i^{n+1})(1 + \frac{m_e}{m_i} q_i^2)\boldsymbol{E}^{n+1} + \frac{m_e}{m_i}\frac{1}{\beta_e} \bigtriangledown \times (\bigtriangledown \times \boldsymbol{E}^{n+1}) \\
= &-(1 + \frac{m_e}{m_i} q_i)\delta \boldsymbol{j}_i^{n+1} \times (\boldsymbol{B}_0 + \delta \boldsymbol{B}^{n+1}) + \frac{1}{\beta_e}(\bigtriangledown \times \delta \boldsymbol{B}^{n+1}) \times \boldsymbol{B}_0 \\
&+ \frac{1}{\beta_e}(\bigtriangledown \times (\boldsymbol{B}_0 + \delta \boldsymbol{B}^{n+1})) \times \delta \boldsymbol{B}^{n+1} + \frac{\eta}{\beta_e}(1 + \frac{m_e}{m_i} q_i^2)(n_{i0} + \delta n_i^{n+1}) \bigtriangledown \times \delta \boldsymbol{B}^{n+1} \\
&- \bigtriangledown \delta n_i^{n+1} + \frac{m_e}{m_i} q_i \bigtriangledown \cdot P_i^{n+1},
\end{aligned}$$

Ion current and nonlinear terms

- The first term on the right hand side of the generalized Ohm's law involves the future ion current density

$$en_i(1+\frac{m_e}{m_i}\frac{q_i^2}{e^2})\boldsymbol{E}^{n+1}+\cdots=-(1+\frac{m_e}{m_i}\frac{q_i}{e})\,\delta\boldsymbol{j}_i^{n+1}\times\boldsymbol{B}^{n+1}+\cdots$$

we approximate $\delta\boldsymbol{j}_i^{n+1}$ as follows

$$\begin{aligned}\delta\boldsymbol{j}_i^{n+1} &= q_i\sum_j w_j^{n+1}\boldsymbol{v}_j^{n+1}\\ &= \delta\boldsymbol{j}_i^{\star}+q_i\,\theta\,\Delta t\sum_j\frac{q_i}{T_i}\boldsymbol{E}^{n+1}(\boldsymbol{x}_j^{n+1})\cdot\boldsymbol{v}_j^{n+1}\boldsymbol{v}_j^{n+1}\\ &\simeq \delta\boldsymbol{j}_i^{\star}+\theta\,\Delta t\,\frac{q_i^2}{m_i}\,\boldsymbol{E}^{n+1}\equiv\boldsymbol{J}_i'.\end{aligned}$$

- For accuracy issues, we iterate on the differences between $\delta\boldsymbol{j}_i^{n+1}$ and $\boldsymbol{J}_i'$.
- For every k_y and k_z mode, the generalized Ohm's law is solved in x direction using finite difference. The equilibrium part is solved by direct matrix inversion. And the nonlinear terms are treated iteratively.

Convergence of the field solver

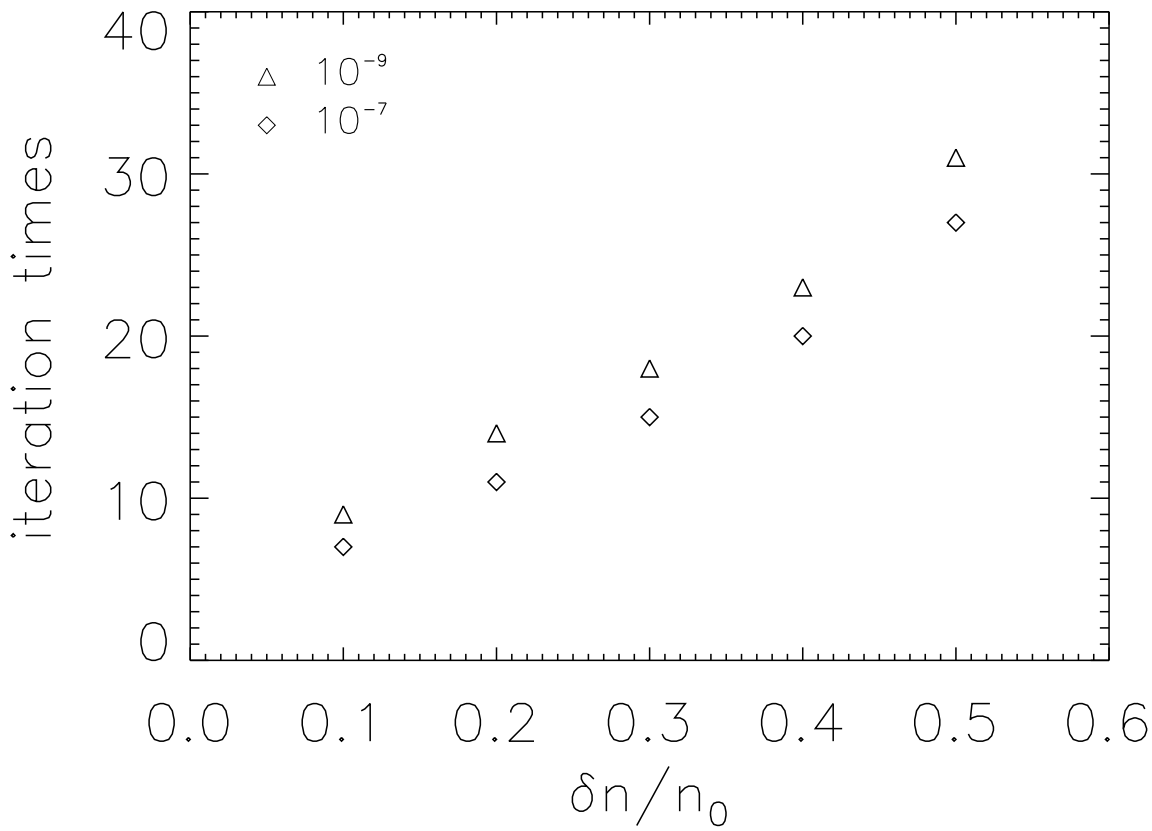

The iteration times needed for field solver to converge to an accuracy order of $\Delta \boldsymbol{E}_x/\boldsymbol{E}_x = 10^{-9}$ (Triangles) and 10^{-7} (Diamonds).

Shear and compressional Alfven waves

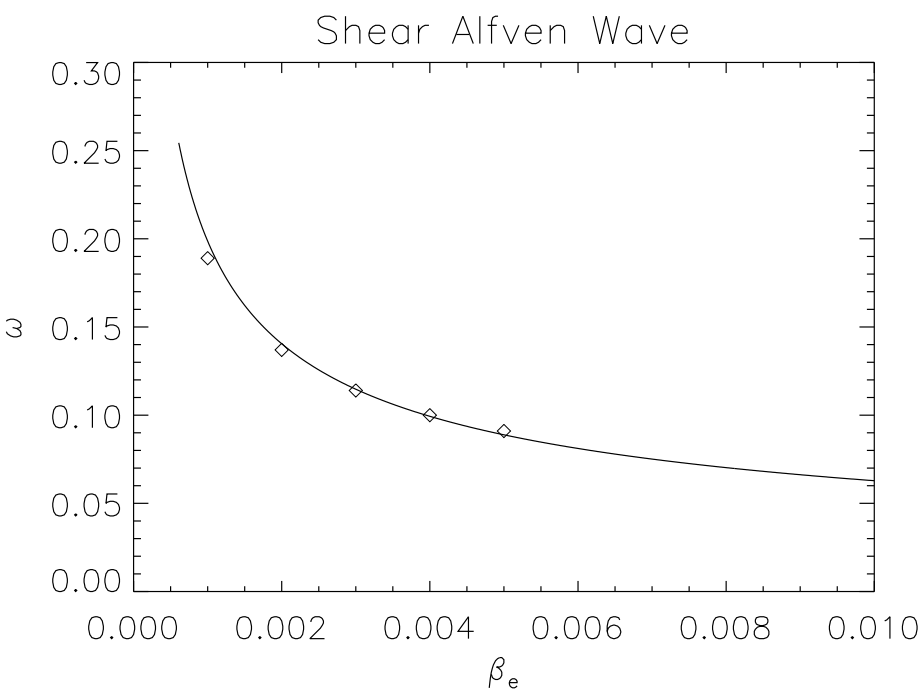

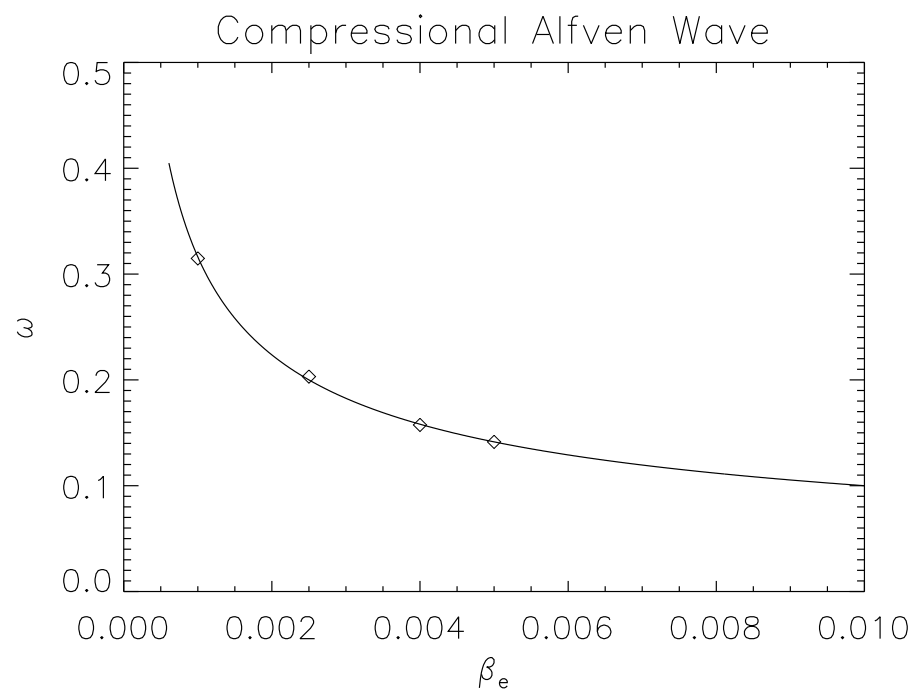

$2 \times 32 \times 32$ grids, 131072 particles.

For shear Alfven wave, $k_\perp = 0$, $k_\parallel \rho_i = 0.00628$, initialize with $\delta \boldsymbol{B}_\perp$.

For compressional Alfven wave, $k_\parallel = 0$, $k_\perp \rho_i = 0.01$, initialize with $\delta \boldsymbol{B}_\parallel$.

These simulations are done in a tilted B_0 field.

Ion acoustic wave and ion Landau damping

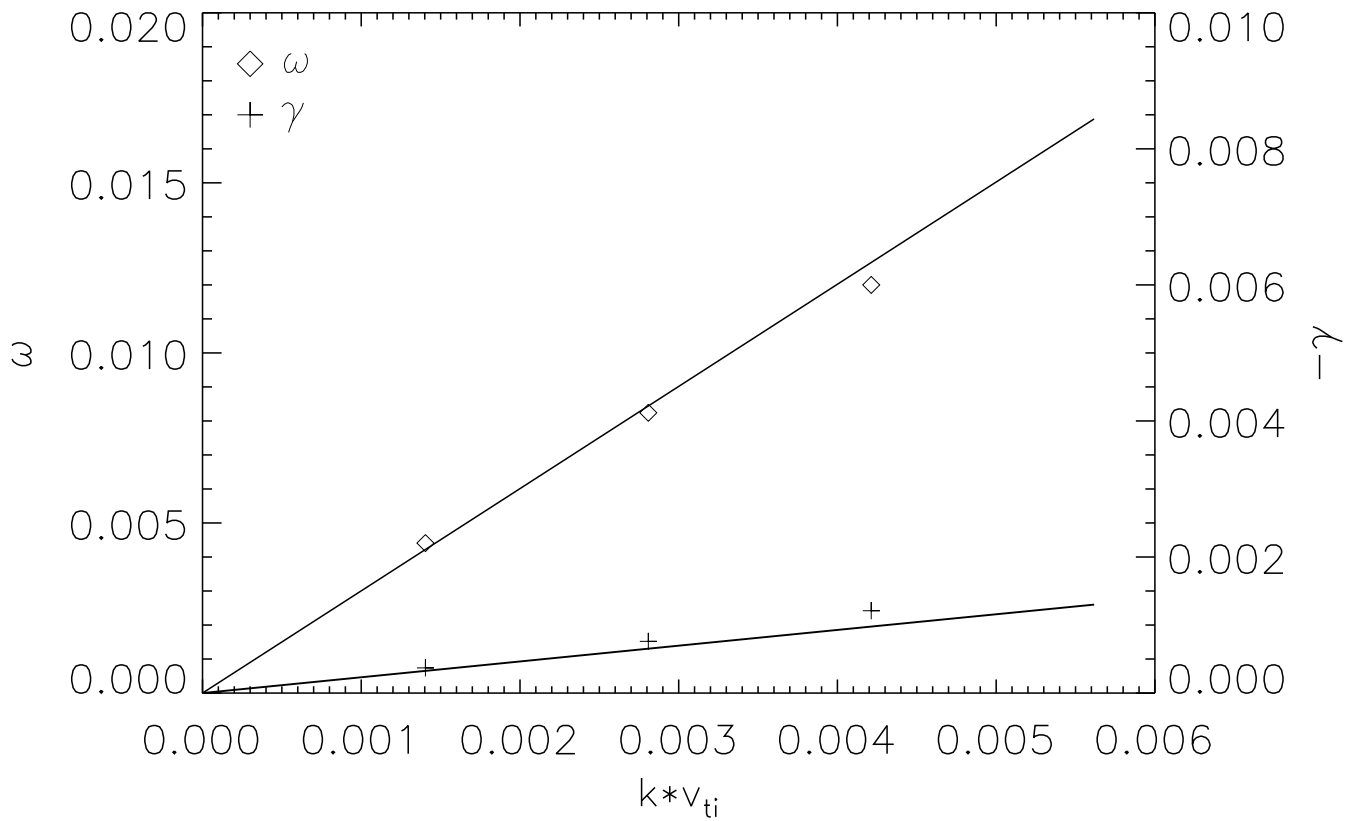

$2 \times 32 \times 32$ grids, 131072 particles. $k_\perp = 0$.

Numerical damping associated with the implicit time advance

- By neglecting ion current and electron inertia, we can study the whistler wave. And the Ohm's law is simplified as

$$\boldsymbol{E} = \frac{1}{\beta_e}(\bigtriangledown \times \delta \boldsymbol{B}) \times \boldsymbol{B}_0.$$

- Getting rid of the particle ion effects makes it easy to perform a Von Neumann stability analysis. Assuming $\Delta t \ll 1$, the numerical dispersion relation can be simplified by neglecting terms with an order of $(\Delta t)^2$ or higher.

$$\begin{cases} \omega_r = \dfrac{k^2}{\beta_e}, \\ \gamma = (\dfrac{1}{2} - \theta)(\dfrac{k^2}{\beta_e})^2 \Delta t. \end{cases}$$

Numerical damping of the whistler wave

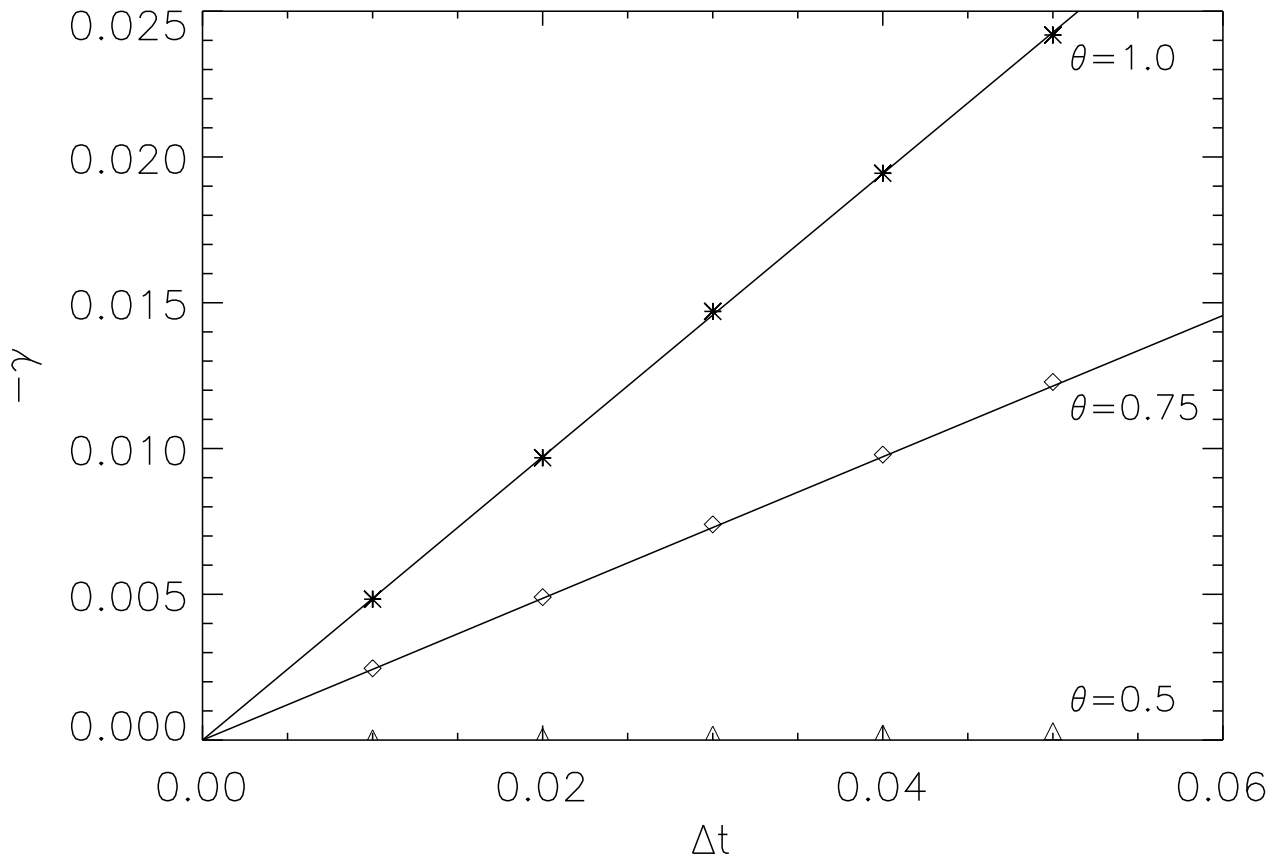

$16 \times 16 \times 32$ grids, 131072 particles, $k_\perp = 0, k_\parallel \rho_i = 0.0628, \beta = 0.004.$

Harris sheet equilibrium

- Zero-order magnetic field $\boldsymbol{B}_0$

$$\boldsymbol{B}_0(\boldsymbol{x}) = B_{y0} \tanh(\frac{x}{a})\ \hat{\boldsymbol{y}} + B_G\ \hat{\boldsymbol{z}}$$

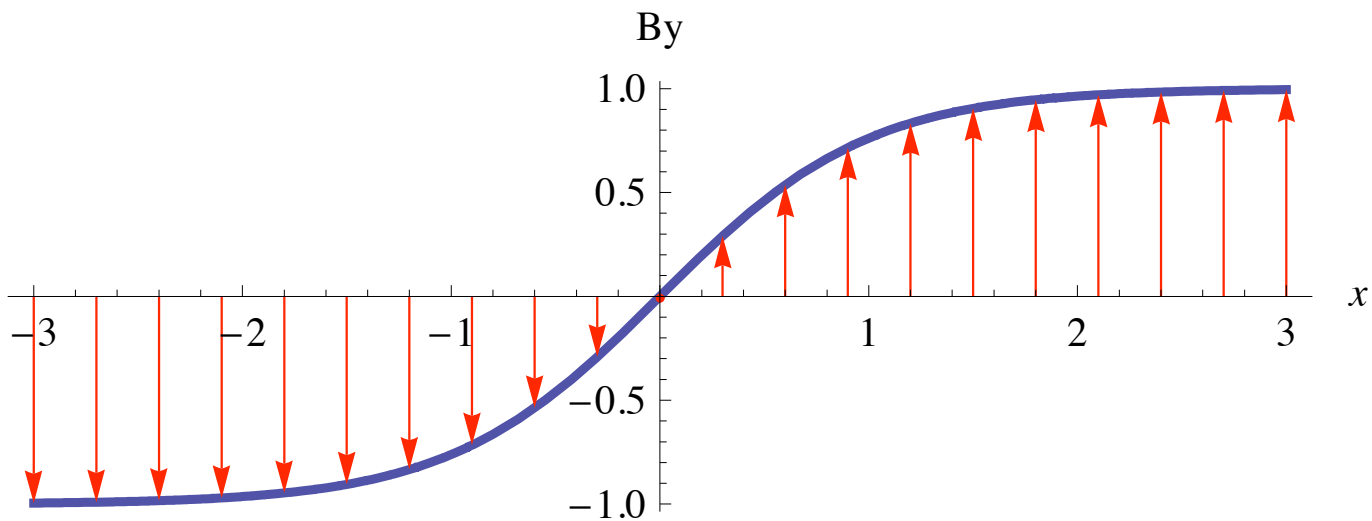

- The equilibrium distribution function is

$$f_{0s} = n_{h0}\ \mathrm{sech}^2(\frac{x}{a}) \left(\frac{2\pi T_s}{m_s}\right)^{-\frac{3}{2}} \exp\left[-\frac{m(v_x^2 + v_y^2 + (v_z - v_{ds})^2)}{2T_s}\right]$$

$$+n_b \left(\frac{2\pi T_s}{m_s}\right)^{-\frac{3}{2}} \exp\left(-\frac{mv^2}{2T_s}\right),$$

- Using Ampere's law $\nabla \times \boldsymbol{B}_y = en_h(v_{di} - v_{de})$, the pressure balance $B_{y0}^2/2\mu_0 = n_{h0}\,(T_i + T_e)$ holds.

- Load particles as $g_0 = (2\pi T_{i0}/m_i)^{-3/2} \exp(-mv^2/2T_{i0})$, the ion equation of motion and weight equation

$$
\begin{aligned}
\frac{d\boldsymbol{v}_i}{dt} &= \frac{q_i}{m_i}(\boldsymbol{E} + \boldsymbol{v}_i \times \boldsymbol{B} - \frac{\eta}{\mu_0} \nabla \times \delta \boldsymbol{B}) \\
\frac{d\boldsymbol{x}_i}{dt} &= \boldsymbol{v}_i \\
\frac{dw_i}{dt} &= \frac{q_i}{T_i} \left((\boldsymbol{E} - \frac{\eta}{\beta_e} \nabla \times \boldsymbol{B}) \cdot \boldsymbol{v}_i (\frac{f_h}{g_0} + n_b) \right. \\
&\quad \left. - \boldsymbol{v}_d \cdot (\boldsymbol{E} + \boldsymbol{v}_i \times \delta \boldsymbol{B} - \frac{\eta}{\beta_e} \nabla \times \boldsymbol{B}) \frac{f_h}{g_0} \right)
\end{aligned}
$$

where the last term in the first equation is to maintain momentum balance.

E. V. Belova *et al*, Plasmas Phys. **7**, 4996 (2000)

Boundary conditions

- Perfect conducting wall boundary condition is employed in x while periodic boundary conditions in y and z direction.

$$\boldsymbol{E}_{y,z}\big|_{x=\pm l_x/2} = 0$$
$$\delta\boldsymbol{B}_x\big|_{x=\pm l_x/2} = 0$$

- Numerically, the boundary condition for $\boldsymbol{E}$ is treated using linear interpolation

$$\frac{\boldsymbol{E}_{y,z}^{-1} + \boldsymbol{E}_{y,z}^{1}}{2} = 0$$
$$\frac{\boldsymbol{E}_{x}^{-1} + \boldsymbol{E}_{x}^{1}}{2} = \boldsymbol{E}_{x}^{0}$$

  at $x = \pm l_x/2$.

- Boundary condition for $\delta\boldsymbol{B}$ is assumed in Faraday's equation.

Island and eigenmode structure

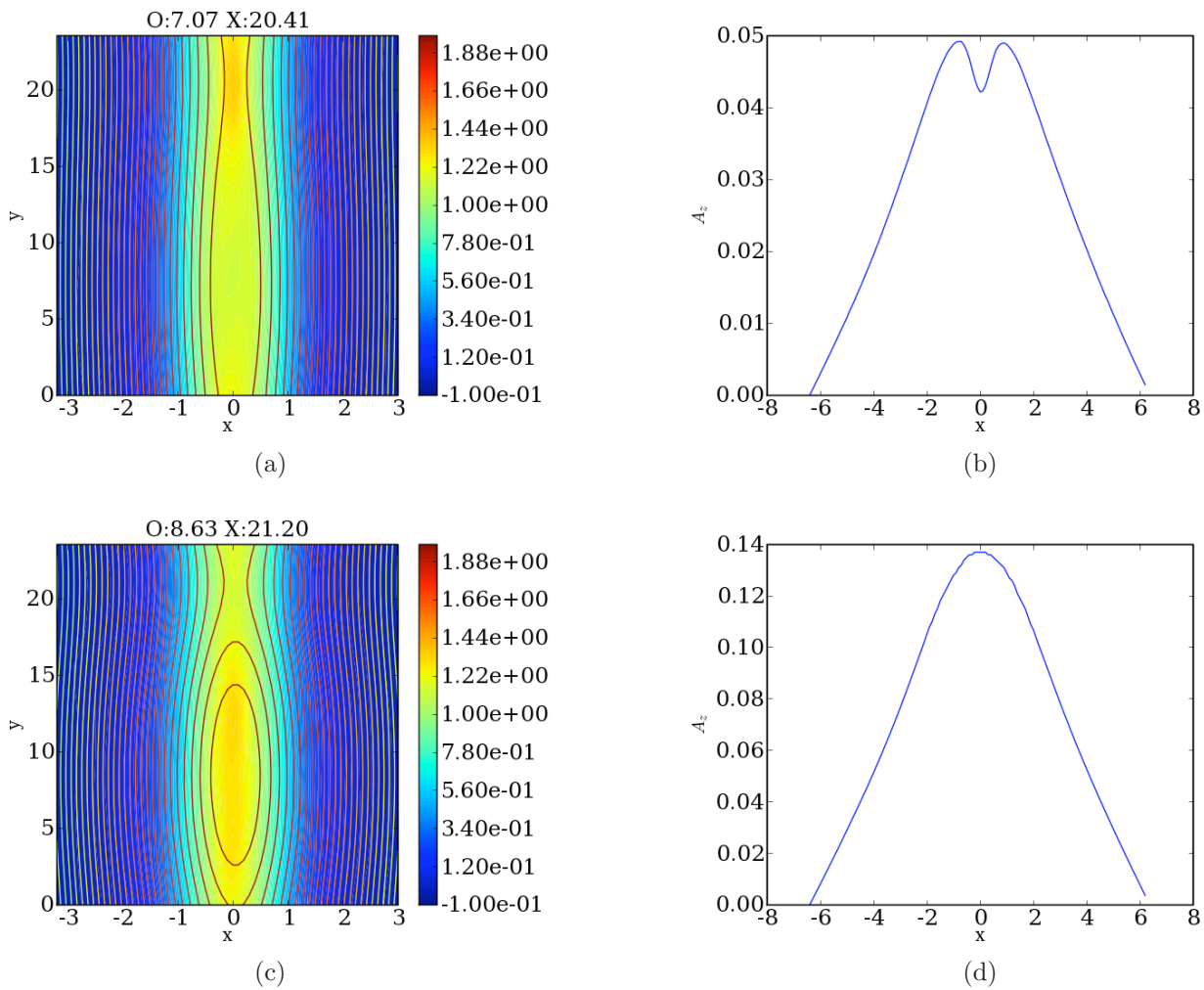

(a)(b) $t = 233\Omega_i^{-1}$, (c)(d) $t = 495\Omega_i^{-1}$ $128 \times 32 \times 64$ grids, 8388608 particles. $\frac{a}{\rho_i} = 1.0, \beta_e = \frac{\mu_0 n_0 T_e}{B_0^2} = 0.5,$
$\eta \frac{e n_0}{B_0} = 15 \times 10^{-4}, \frac{\boldsymbol{B}_G}{B_0} = 0, \frac{T_i}{T_e} = 1, \frac{l_x}{\rho_i} = 12.8, \frac{l_y}{\rho_i} = 25.12$

Convergence of mesh sizes

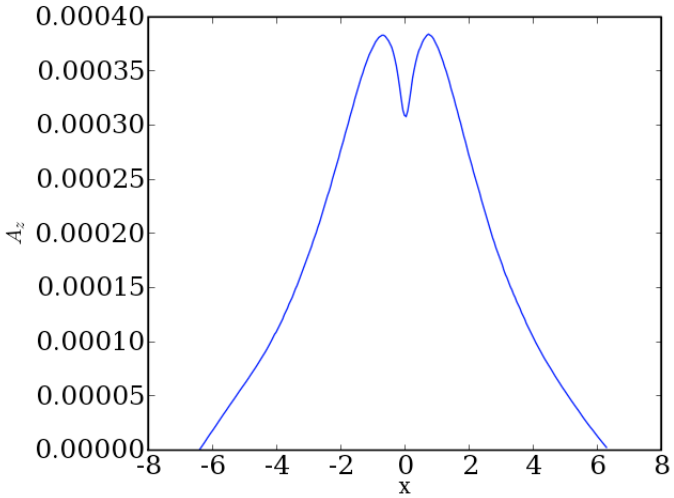

(a)

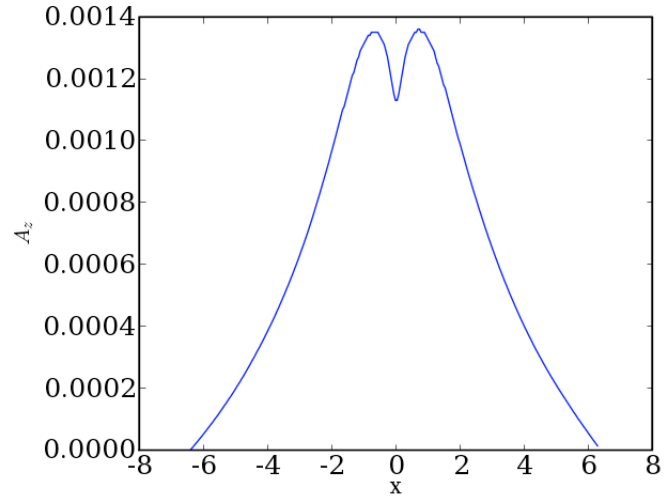

(b)

(a) $128 \times 32 \times 64$ (b) $256 \times 32 \times 64$.

$\frac{a}{\rho_i} = 1.0, \beta_e = \frac{\mu_0 n_0 T_e}{B_0^2} = 0.5, \eta \frac{e n_0}{B_0} = 15 \times 10^{-4}, T_i/T_e = 1.0, \frac{l_x}{\rho_i} = 12.8, \frac{l_y}{\rho_i} = 25.12.$

The linear growth rate vs η

- Linear Tearing mode theory shows that the growth rate is (scaled)

$$\gamma = \; 0.55 \; (\frac{1}{\beta})^{1/5} \; \Delta'^{4/5} \eta^{3/5} \; (k \; B'_{y0})^{2/5}.$$

$$\Delta' = \; \frac{2}{a}(\frac{1}{ka} - ka)\frac{ka - \tanh(l_x/2a)\tanh(kl_x/2)}{ka\tanh(kl_x/2) - \tanh(l_x/2a)}.$$

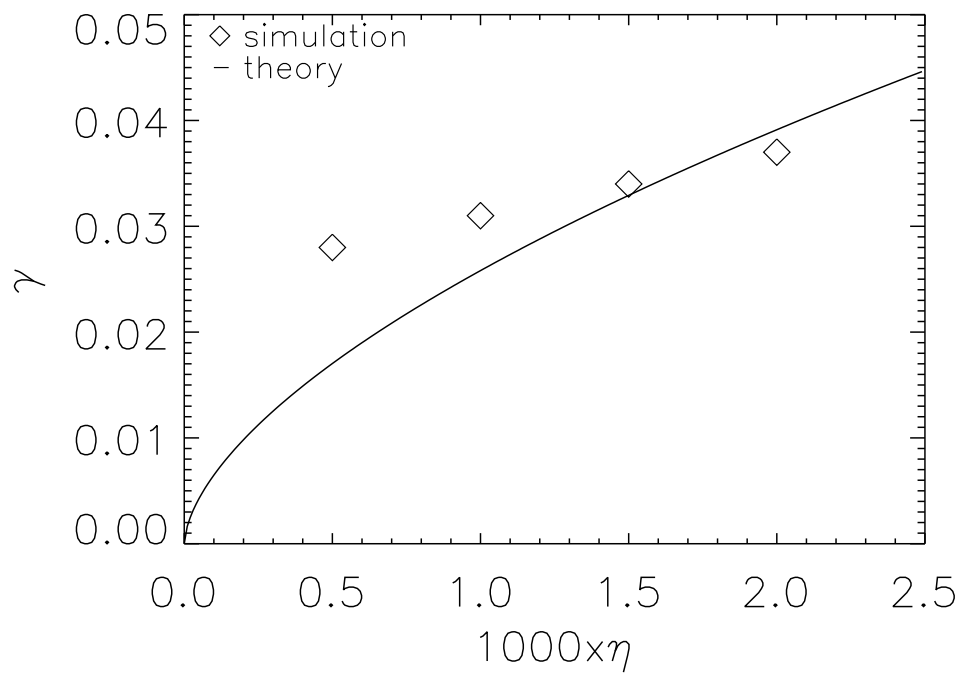

$128 \times 32 \times 64$ grids, 8388608 particles. $\frac{a}{\rho_i} = 1.0, \beta_e = \frac{\mu_0 n_0 T_e}{B_0^2} = 0.5, \; \frac{\boldsymbol{B}_G}{B_0} = 0, \frac{T_i}{T_e} = 1, \frac{l_x}{\rho_i} = 12.8, \frac{l_y}{\rho_i} = 18.84$

The linear growth rate vs k

- Linear Tearing mode theory shows that the growth rate is (scaled)

$$\gamma = \; 0.55 \; (\frac{1}{\beta})^{1/5} \; \Delta'^{4/5} \eta^{3/5} \; (k \; B'_{y0})^{2/5}.$$

$$\Delta' = \; \frac{2}{a}(\frac{1}{ka} - ka)\frac{ka - \tanh(l_x/2a)\tanh(kl_x/2)}{ka\tanh(kl_x/2) - \tanh(l_x/2a)}.$$

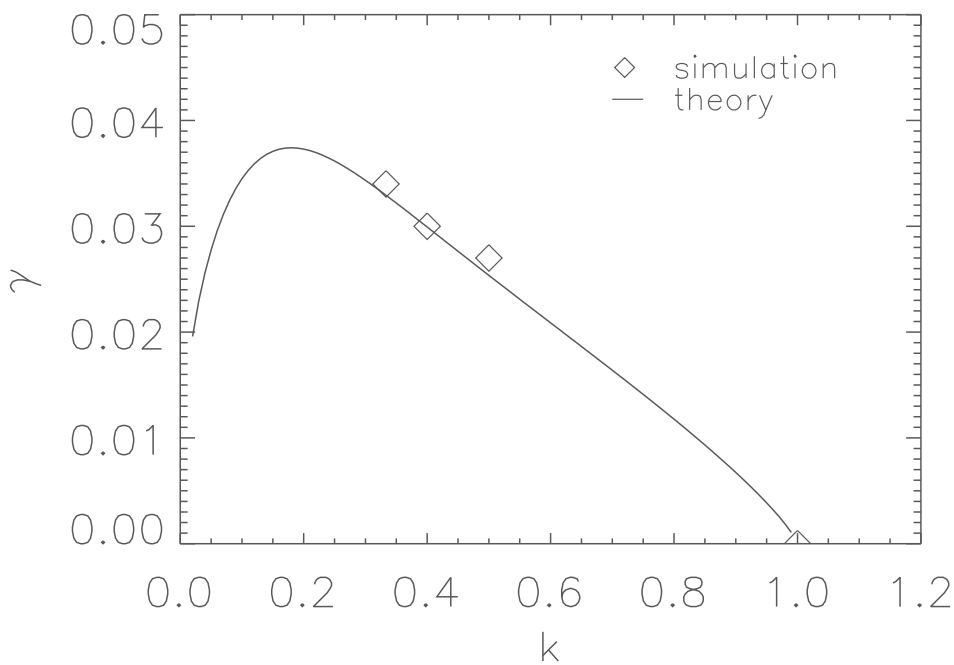

$128 \times 32 \times 64$ grids, 8388608 particles. $\frac{a}{\rho_i} = 1.0, \beta_e = \frac{\mu_0 n_0 T_e}{B_0^2} = 0.5, \frac{\boldsymbol{B}_G}{B_0} = 0, \frac{T_i}{T_e} = 1, \frac{l_x}{\rho_i} = 12.8, \eta = 0.0015$

Full evolution with different Δ'

- Tearing mode evolution with different Δ',

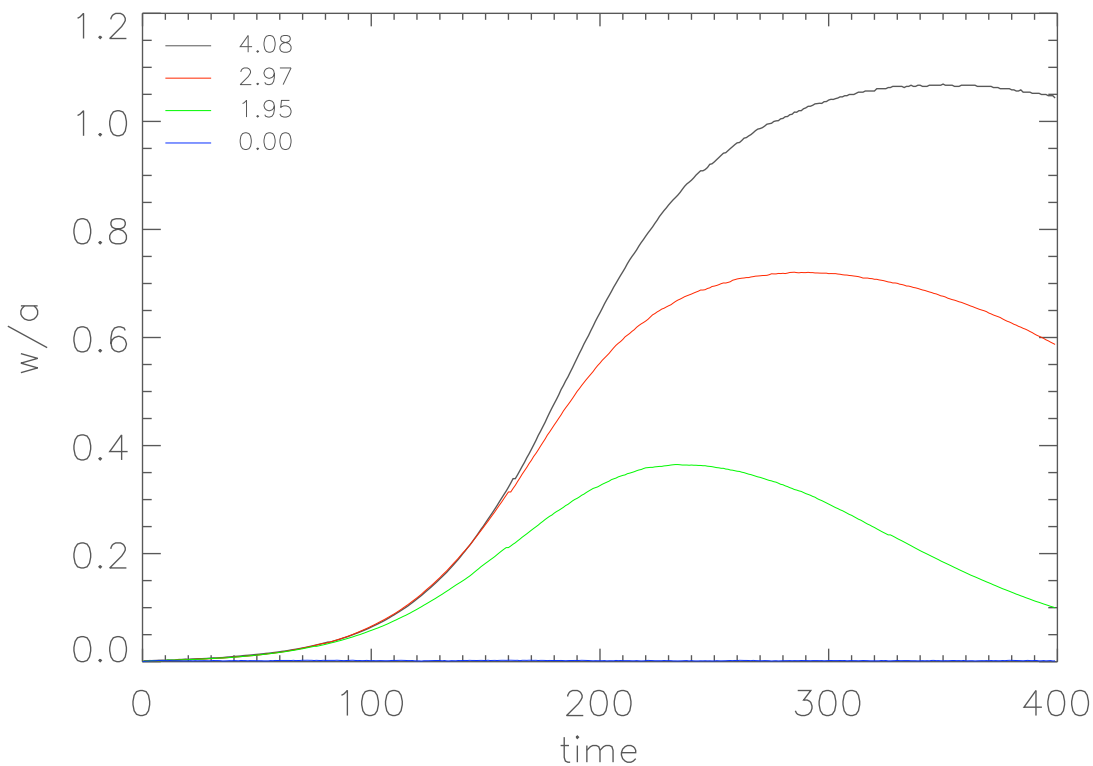

$128 \times 32 \times 64$ grids, 8388608 particles. $\frac{a}{\rho_i} = 1.0, \beta_e = \frac{\mu_0 n_0 T_e}{B_0^2} = 0.5, \frac{\boldsymbol{B}_G}{B_0} = 0, \frac{T_i}{T_e} = 1, \frac{l_x}{\rho_i} = 12.8, \eta = 0.0015$

Rutherford stage

- Island growth can be described by $\frac{dw}{dt} = 1.22\eta(\Delta' - \alpha' w)$, which reduces to the Rutherford equation when w is small ($\alpha' = 0.82$ in this case).

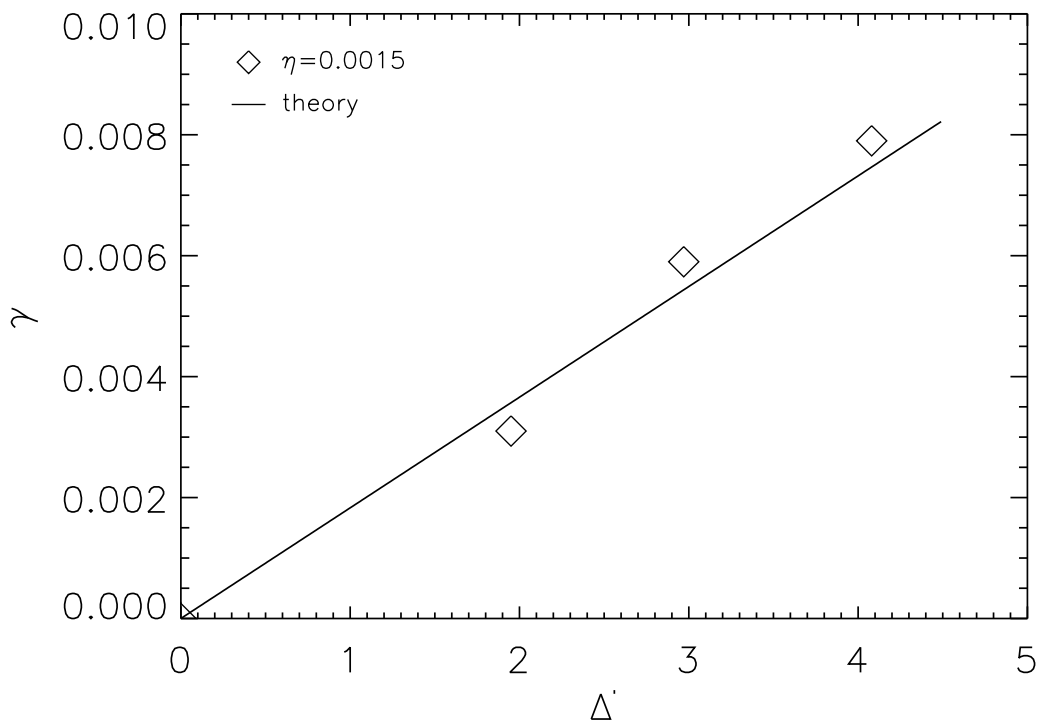

$128 \times 32 \times 64$ grids, 8388608 particles. $\frac{a}{\rho_i} = 1.0, \beta_e = \frac{\mu_0 n_0 T_e}{B_0^2} = 0.5, \frac{\boldsymbol{B}_G}{B_0} = 0, \frac{T_i}{T_e} = 1, \frac{l_x}{\rho_i} = 12.8, \eta = 0.0015$

D. F. Escande and M. Ottaviani, Phys. Lett. A **323**, 278-284(2004)

Saturation

- From the equation $\frac{dw}{dt} = 1.22\eta(\Delta' - \alpha' w)$, the island width at saturation is $w_s = 1.22\Delta'$.

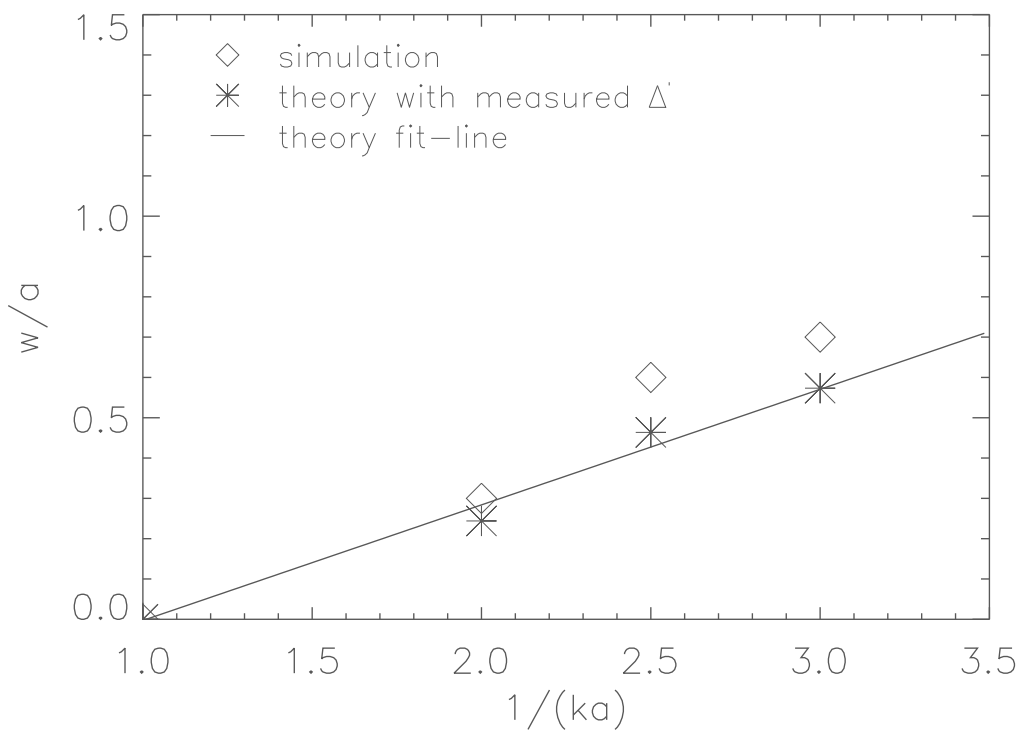

$128 \times 32 \times 64$ grids, 8388608 particles. $\frac{a}{\rho_i} = 1.0, \beta_e = \frac{\mu_0 n_0 T_e}{B_0^2} = 0.5, \frac{\boldsymbol{B}_G}{B_0} = 0, \frac{T_i}{T_e} = 1, \frac{l_x}{\rho_i} = 12.8, \eta = 0.0015$

Island evolution—$\Delta' = 7.875$

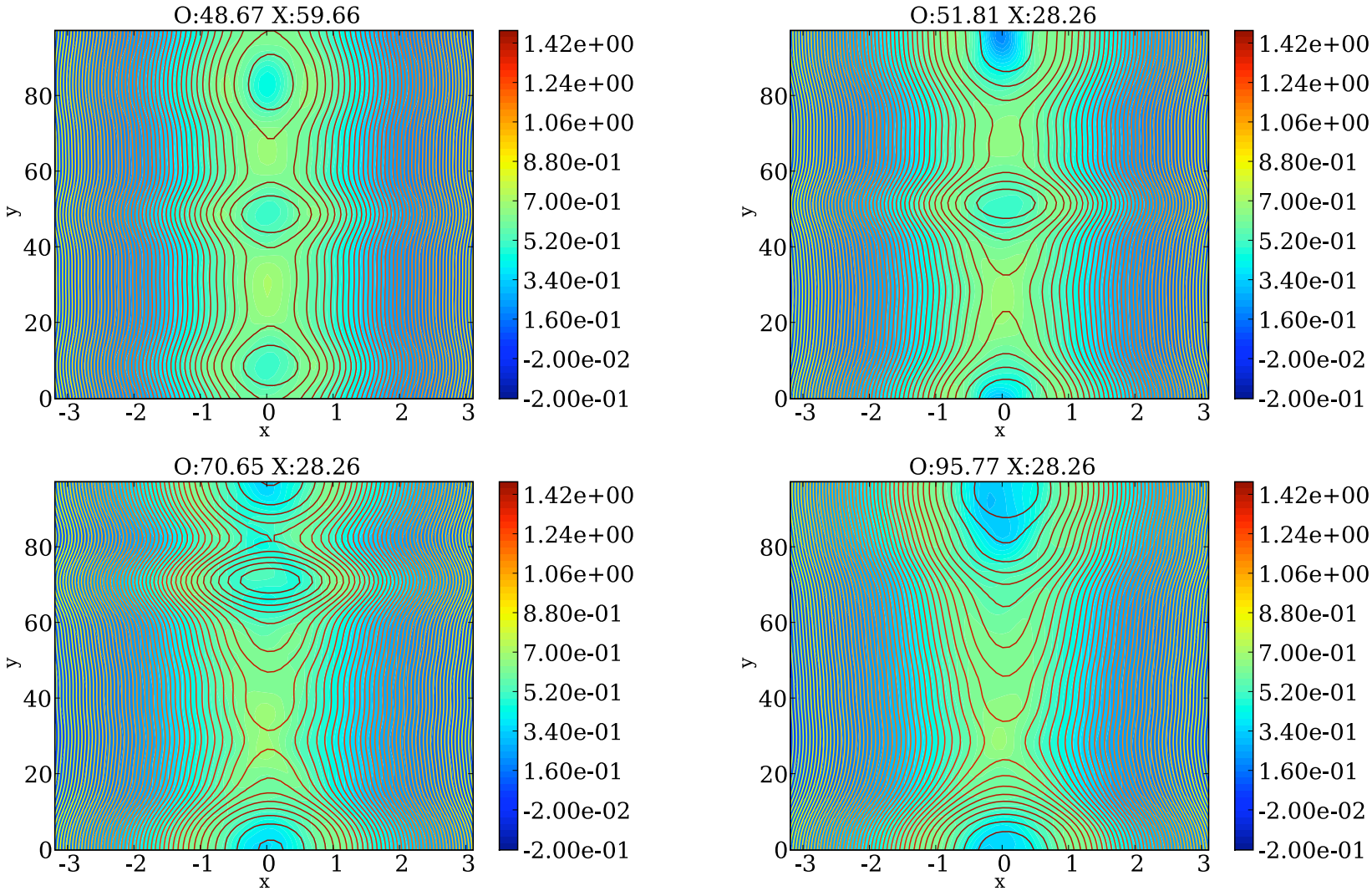

$128 \times 32 \times 64$, 8388608 particles. $\frac{a}{\rho_i} = 1.0, \beta_e = \frac{\mu_0 n_0 T_e}{B_0^2} = 0.5, \eta \frac{e n_0}{B_0} = 0.0015, \frac{\boldsymbol{B}_G}{B_0} = 0, \frac{T_i}{T_e} = 1, \frac{l_x}{\rho_i} = 12.8, \frac{l_y}{\rho_i} = 100.48$

From left to right, top to bottom: $t = 744, 1064, 1532, 1776\ \Omega_i^{-1}$

Summary

1. We have implemented a second-order accurate implicit algorithm with Lorentz force ions and isothermal fluid electrons which is
   - Quasi-neutral and fully electromagnetic.
   - Suitable for MHD scale plasmas.

2. Demonstrated 3-D slab simulation for Alfvèn waves, whistler wave, and the ion acoustic wave. Showed that the time-centered second order scheme brings no numerical damping through whistler waves studies.

3. The full evolution of resistive tearing mode is investigated with Harris sheet equilibrium.

4. We are working on large Δ' tearing mode and exploring detailed role played by particle ions.

Measurement of the Δ'

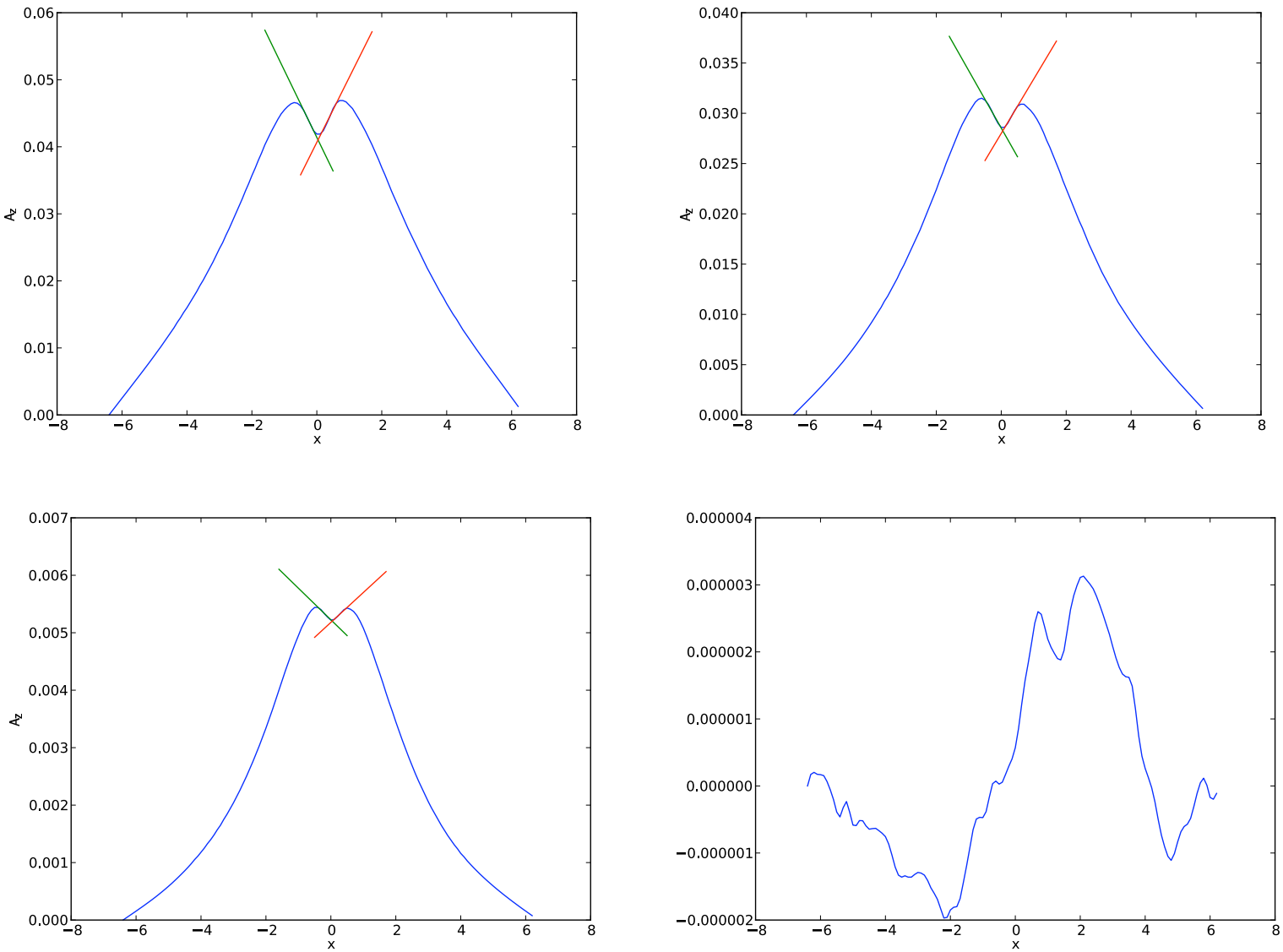

$128 \times 32 \times 64$ grids, 8388608 particles. $\frac{a}{\rho_i} = 1.0, \beta_e = \frac{\mu_0 n_0 T_e}{B_0^2} = 0.5, \frac{\boldsymbol{B}_G}{B_0} = 0, \frac{T_i}{T_e} = 1, \frac{l_x}{\rho_i} = 12.8, \eta = 0.0015$